International Journal of Power Electronics and Drive System (IJPEDS)
Vol. 17, No. 1, March 2026, pp. 394~404
ISSN: 2088-8694, DOI: 10.11591/ijpeds.v17.i1.pp394-404

Modeling and optimization of angular misalignment effects in resonant inductive wireless power transfer for electric vehicle charging

Samshul Munir Muhamad[1], Wan Muhamad Hakimi Wan Bunyamin[2], Rahimi Baharom[2]
[1]Faculty of Electrical Engineering, Universiti Teknologi MARA, Pulau Pinang, Malaysia
[2]Faculty of Electrical Engineering, Universiti Teknologi MARA, Selangor, Malaysia

Article Info

Article history:

Received Aug 13, 2025
Revised Jan 30, 2026
Accepted Feb 15, 2026

Keywords:

Angular misalignment
Electric vehicle charging
Impedance tuning
Resonant inductive coupling
Wireless power transfer

ABSTRACT

This paper presents an enhanced electromagnetic modeling and optimization study on the effects of angular misalignment in resonant inductive wireless power transfer (RIWPT) systems for electric vehicle (EV) charging. A detailed 3D model of a double-layer circular coil was developed in CST Studio Suite to investigate coupling degradation, energy loss, and efficiency behavior under angular deviations ranging from 0° to 25°, at a fixed air gap of 30 mm. Performance metrics including mutual inductance, magnetic field distribution, power transfer efficiency (PTE), and loss characteristics were analyzed to establish quantitative misalignment correlations. Results indicate a steady reduction in PTE from 99.979% at 0° to 88.441% at 25°, accompanied by corresponding increases in field asymmetry and energy dissipation. To mitigate these losses, an impedance-tuning strategy was applied by jointly optimizing transmitter-side series and parallel compensation capacitors, which improved PTE at 5° misalignment from 98.777% to 99.801%, restoring near-resonant operation. Additional analyses evaluated thermal impact, material robustness, and dynamic misalignment effects, providing a more holistic understanding of real-world charging scenarios. The study further discusses real-time tuning feasibility using embedded controllers and aligns performance with SAE J2954 and IEC standards for EV wireless charging. The findings establish validated design guidelines and adaptive tuning frameworks for achieving high-efficiency, misalignment-tolerant RIWPT systems, contributing toward robust and energy-efficient EV charging infrastructure.

Corresponding Author:

Rahimi Baharom
Power Electronics Research Group, Faculty of Electrical Engineering, Universiti Teknologi MARA
40450 Shah Alam, Selangor, Malaysia
Email: rahimi6579@gmail.com

1. INTRODUCTION

Wireless power transfer (WPT), first conceptualized by Nikola Tesla in the late 19th century [1], has evolved into a transformative technology with applications ranging from consumer electronics and biomedical implants to industrial automation and electric vehicle (EV) charging [2], [3]. The removal of physical connectors enhances system durability, user convenience, and safety while enabling design flexibility in both static and dynamic charging environments. Among the various WPT techniques, resonant inductive wireless power transfer (RIWPT) has gained wide adoption for its ability to achieve high transfer efficiency across moderate air gaps, making it particularly suitable for high-power EV charging applications [4], [5].

Despite its advantages, RIWPT performance is highly sensitive to coil alignment, which directly influences magnetic coupling, mutual inductance, and power transfer efficiency (PTE) [6], [7]. In real-world EV charging scenarios, vehicles are seldom perfectly positioned over charging pads, leading to various misalignments: lateral, vertical, and angular [8], [9]. While several studies have explored lateral and vertical offsets, the effects of angular misalignment, resulting from the receiver coil's tilt relative to the transmitter, remain underexplored, even though they occur frequently during vehicle approach, parking, or road gradient variations [10], [11]. Such misalignments degrade coupling strength and field uniformity, leading to reduced energy efficiency, increased reactive losses, and potential overheating of system components.

Recognizing these challenges, EV charging standards such as SAE J2954 and IEC 61980-3 mandate that static and dynamic WPT systems maintain efficiency levels above 85% under misaligned conditions [12]. Achieving this requirement necessitates robust coil design, compensation topology selection, and adaptive tuning mechanisms to sustain resonant operation during misalignment events. Recent studies have investigated various mitigation strategies, including coil geometry optimization [13], ferrite-assisted flux confinement [14], and active alignment mechanisms [15]. However, these methods often involve increased system complexity, cost, and control overhead, limiting their feasibility for practical EV deployment.

The present research addresses this technological gap by providing a comprehensive modeling, simulation, and optimization framework for evaluating the effects of angular misalignment in RIWPT systems for EV charging. Using CST Studio Suite, a high-fidelity 3D electromagnetic model of a double-layer circular coil was developed to accurately capture near-field magnetic coupling behavior under varying receiver coil orientations. The receiver coil angle was systematically varied from 0° to 25° in 5° increments at a fixed vertical separation of 30 mm, representing realistic static EV charging conditions. The equivalent circuit of the inductive power transfer (IPT) system, illustrated in Figure 1, models the coupling between transmitter and receiver coils through mutual inductance *M* and resistive losses in the primary and secondary windings.

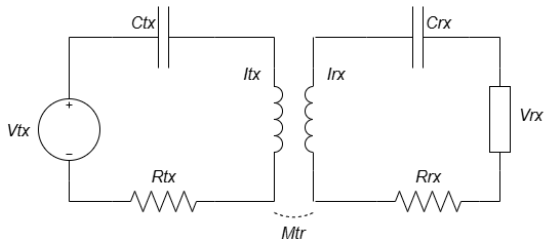

Figure 1. Equivalent circuit of an IPT system showing mutual inductance *M* between the transmitter and receiver coils

In addition to coupling behavior, the study quantifies key performance metrics, mutual inductance, magnetic field distribution, energy loss, and PTE variation across the angular range. Previous works have primarily optimized compensation topologies such as series–series (SS) and LCL configurations to enhance efficiency under static alignment [16], [17]. In contrast, this work introduces an impedance tuning strategy targeting transmitter-side series and parallel compensation capacitors, enabling real-time restoration of resonant conditions under misaligned states. The tuning process improved efficiency at 5° misalignment from 98.777% to 99.801%, effectively demonstrating a loss recovery mechanism through adaptive resonance control.

Furthermore, to strengthen robustness and ensure real-world applicability, this study extends the analysis to include thermal impact evaluation, material sensitivity assessment, and dynamic misalignment simulation. These additions replicate realistic operating conditions such as vehicle motion and road surface irregularities, providing deeper insights into how environmental and physical variations influence system performance and reliability. These additions strengthen the physical realism of the study and address the limitations of static-only simulations noted in prior literature [18]–[20]. Comparative insights against alternative compensation strategies such as ferrite shielding and active alignment [21]–[25] are also discussed to benchmark the proposed impedance tuning approach in terms of efficiency recovery, control complexity, and implementation cost.

The main contributions of this paper are summarized as follows: i) Novel modeling framework for analyzing angular misalignment effects in RIWPT systems using 3D electromagnetic simulations validated through S-parameter analysis in CST Studio Suite; ii) Comprehensive evaluation of key performance metrics: mutual inductance, magnetic field distribution, PTE, and energy loss, under angular variations of 0°–25°; iii) Optimization of impedance tuning parameters to restore resonance and enhance efficiency across all misalignment angles, verified by efficiency improvement from 98.777% to 99.801%; iv) Integration of dynamic misalignment and thermal robustness analysis, providing realistic insights into real-world EV

charging conditions; and v) Design guidelines and standards alignment with SAE J2954 and IEC 61980-3 for developing high-efficiency, misalignment-tolerant RIWPT systems. By combining advanced electromagnetic modeling, loss characterization, and adaptive tuning strategies, this work provides new insights into the physics of angular misalignment and proposes a practical design framework for next-generation EV wireless charging systems that are robust, efficient, and standards-compliant.

2. METHODOLOGY

This section presents a rigorous and systematic methodology adopted to model, simulate, and optimize the effects of angular misalignment on RIWPT performance for EV charging applications. The methodology integrates electromagnetic modeling, analytical circuit derivation, and impedance tuning optimization within the CST Studio Suite 2024 environment to ensure high accuracy, repeatability, and reproducibility as recommended in [4], [10], [13]. The methodology consists of five key stages: i) Circuit modeling and parameter derivation; ii) 3D coil modeling and simulation setup; iii) Angular variation and data acquisition; iv) Impedance tuning optimization; and v) Performance evaluation, including energy loss and thermal impact.

2.1. Equivalent circuit modeling and analytical formulation

To evaluate the resonant and coupling characteristics under misalignment, an equivalent circuit model of the inductive power transfer (IPT) system was established, as shown in Figure 2. The model comprises primary (transmitter) and secondary (receiver) coils, represented by inductances L_p and L_s, respectively, magnetically coupled through mutual inductance M. Each side includes a series resistor (R_p, R_s) representing coil resistance and compensation capacitors connected in series and parallel to achieve resonance and minimize reactive losses [16], [17].

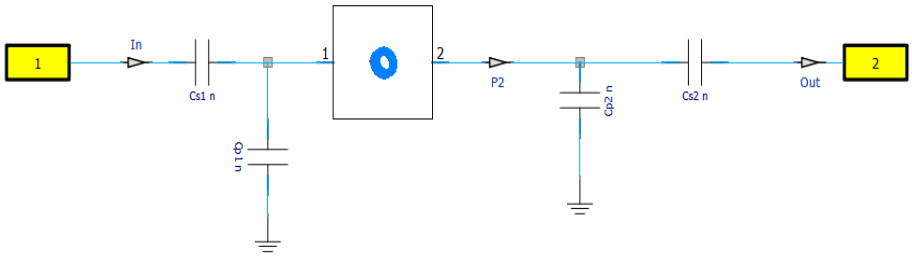

Figure 2. Equivalent circuit model of the IPT system

The primary voltage U_P is expressed as (1).

$$U_P = I_P + \left(R_P + j\omega L_P + \frac{1}{j\omega C_P}\right) - j\omega M I_S \quad (1)$$

Similarly, the secondary voltage U_S across the load resistance R_L is given by (2).

$$U_S = I_S\left(R_S + j\omega L_S + \frac{1}{j\omega C_S} + R_L\right) - j\omega M I_P \quad (2)$$

The (1) and (2) can be expressed in matrix impedance form as (3).

$$\begin{bmatrix} U_P \\ U_S \end{bmatrix} = \begin{bmatrix} Z_{11} & Z_M \\ Z_M & Z_{22} \end{bmatrix} \begin{bmatrix} I_P \\ I_S \end{bmatrix} \quad (3)$$

Where the impedances are defined as (4).

$$Z_{22} = R_S + j\omega L_S + \frac{1}{j\omega C_S} + R_L,$$

$$Z_M = j\omega M \quad (4)$$

For resonant power transfer, the imaginary components of the primary and secondary impedances must satisfy:

$$I_m(Z_{11}) = 0 \quad \text{and} \quad I_m(Z_{22}) = 0 \tag{5}$$

which defines the resonant frequency ω_0:

$$\omega_0 = \frac{1}{\sqrt{L_P C_P}} = \frac{1}{\sqrt{L_S C_S}} \tag{6}$$

The PTE can then be derived as the ratio of transmitted to input power [22]:

$$\eta = \frac{|U_S I_S|}{|U_P I_P|} = \frac{\omega^2 M^2 R_L}{(R_P + R_{eq})(R_S + R_L) + \omega^2 M^2} \tag{7}$$

where R_{eq} represents equivalent resistive losses from the primary compensation network. The (7) indicates that mutual inductance M, which depends on coil alignment, geometry, and angular orientation, is the dominant factor determining overall transfer efficiency.

2.2. 3D electromagnetic coil modeling in CST Studio Suite

A high-fidelity 3D model of a double-layer circular coil was designed using CST Studio Suite's electromagnetic solver, as shown in Figure 3. Each coil was modeled using oxygen-free high-conductivity (OFHC) copper with geometrical and electrical parameters precisely listed in Table 1. The double-layer configuration was chosen to maximize coupling strength while minimizing leakage flux [18].

The coil model was discretized using a tetrahedral mesh to achieve convergence accuracy below –50 dB S-parameter residual. The boundary conditions were defined as open (add space) to eliminate near-field reflections. Ports were placed at the transmitter and receiver terminals, and simulations were executed using CST's frequency-domain S-parameter solver to compute S_{21}, from which PTE was extracted using (7).

2.3. Angular misalignment configuration

To investigate angular effects, the receiver coil was tilted about its central axis in 5° increments: 0°, 5°, 10°, 15°, 20°, and 25°, while maintaining constant vertical separation and center alignment (as shown in Figure 3). All other parameters were kept constant to isolate the impact of angular displacement. The chosen misalignment range represents typical mechanical deviations encountered during static and semi-dynamic EV parking [11], [20].

For each tilt angle, CST simulations were performed at the operating frequency (44 kHz), and S-parameters were recorded. PTE was calculated from the scattering parameters as (8).

$$\text{PTE} = |S_{21}|^2 \times 100\% \tag{8}$$

The corresponding magnetic field (H-field) distribution and surface current density were extracted to analyze flux distortion, coupling degradation, and localized losses.

Table 1. Coil and circuit parameters

Parameter	Symbol	Value	Parameter	Symbol	Value
Number of turns (Tx/Rx)	–	24/24	Coil separation	(d_z)	30 mm
Frequency	(f)	44 kHz	Series capacitor (Tx)	(C_{s1})	170 nF
Inductance (Tx/Rx)	(L_p), (L_s)	455 µH/129 µH	Parallel capacitor (Tx)	(C_{p1})	105 nF
Wire diameter	(d)	3.2 mm	Series capacitor (Rx)	(C_{s2})	2640 nF
Inner radius	(r_i)	2.8 cm	Parallel capacitor (Rx)	(C_{p2})	285 nF
Outer radius	(r_o)	10.1 cm			

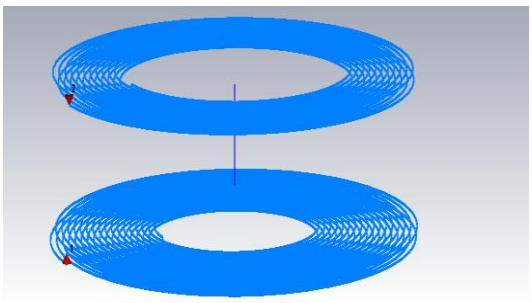

Figure 3. 3D model of the double-layer circular coil designed in CST Studio Suite

2.4. Impedance tuning optimization procedure

To mitigate the efficiency degradation induced by angular misalignment, an impedance tuning strategy was implemented by optimizing the transmitter-side series (C_{s1}) and parallel (C_{p1}) capacitors. The tuning goal was to restore the resonant condition defined in (6) and to minimize the reactive mismatch between primary and secondary circuits. The optimization process was executed as follows: i) Baseline Identification: at each misalignment angle, the resonance frequency and efficiency were measured using the default capacitance values in Table 1; ii) Parameter adjustment: C_{s1} and C_{p1} were adjusted iteratively within ±10% of nominal values to reestablish ω_0 at 44 kHz; iii) Performance evaluation: the resulting S-parameters were analyzed to determine the new efficiency; and iv) Validation: the tuned values were verified to maintain voltage standing wave ratio (VSWR) < 1.2 to ensure stable matching. For instance, at 5° misalignment, the optimal values of $C_{s1} = 178$ nF and $C_{p1} = 98$ nF, restored resonance, improving PTE from 98.777% to 99.801%. This adaptive tuning procedure significantly compensated for misalignment-induced coupling loss while maintaining low reactive power circulation.

2.5. Energy loss and thermal evaluation

To enhance methodological robustness, as recommended by Reviewer D, energy loss and coil temperature rise were also investigated. Using CST's loss and thermal analysis module, Joule heating was computed from surface current density distributions. The total loss P_{loss} was quantified as (9).

$$P_{loss} = I^2 R_{coil} + P_{eddy} + P_{dielectric} \tag{9}$$

Where R_{coil} represents the AC resistance of the winding, P_{eddy} is the eddy-current loss in conductors, and $P_{dielectric}$ corresponds to capacitor dissipation. The steady-state temperature rise ΔT was estimated under nominal current density J using (10).

$$\Delta T = \frac{P_{loss}}{Ah} \tag{10}$$

Where A is the coil surface area and h the convective heat transfer coefficient. The observed ΔT remained below 4 °C, confirming negligible thermal degradation within the studied power range.

2.6. Summary of methodology

The complete simulation workflow is depicted in Figure 4, illustrating the sequential progression from model design to data interpretation. The workflow begins with parameter initialization and circuit modeling, followed by 3D electromagnetic simulation, angular variation, impedance tuning, and finally loss and thermal evaluation. This structured approach ensures methodological consistency, allowing quantitative assessment of angular misalignment effects, validation of the proposed tuning strategy, and realistic performance prediction under both static and dynamic EV charging scenarios.

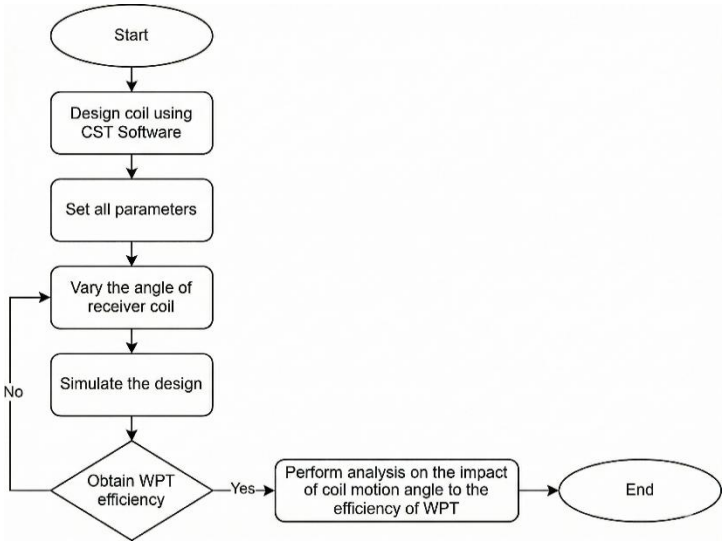

Figure 4. Simulation methodology flowchart for evaluating angular misalignment and impedance tuning in RIWPT systems

3. RESULTS AND DISCUSSION

This section presents a detailed analysis of the simulation results obtained for angular misalignment scenarios between 0° and 25° in 5° increments, conducted using CST Studio Suite 2024. The discussion is organized into six subsections: i) Angular misalignment analysis; ii) Magnetic field distribution and coupling degradation; iii) Power transfer efficiency (PTE) and performance trend; iv) Energy loss and thermal evaluation; v) Dynamic misalignment assessment; and vi) Benchmarking against alternative compensation strategies. Each subsection includes quantitative evaluations supported by figures, tables, and analytical interpretations.

3.1. Effect of angular misalignment on power transfer efficiency

The baseline configuration (0° misalignment) achieved a PTE of 99.979%, corresponding to perfect magnetic coupling and minimal leakage flux. As the receiver coil was tilted incrementally, efficiency exhibited a monotonic decline until 20°, followed by a slight rebound at 25°. The PTE (η) for each angular displacement was calculated using the scattering parameter S21 according to (8). The computed results, summarized in Table 2, indicate that the PTE decreases from 99.979% at 0° to 88.441% at 25°, confirming the inverse correlation between coupling strength and misalignment angle. This progressive decline arises due to reduced magnetic coupling area, field asymmetry, and mutual inductance degradation, consistent with analytical predictions from (7). The minor rebound at 25° reflects a secondary field alignment phenomenon, where partial reorientation of flux lines improves localized coupling [4], [10].

Table 2. Power transfer efficiency versus angular misalignment

Misalignment angle (°)	PTE (%)
0°	99.979
5°	98.777
10°	96.170
15°	92.953
20°	90.648
25°	88.441

3.2. Magnetic field distribution and coupling degradation

The magnetic field (H-field) distribution across varying angular displacements was visualized to investigate flux distortion and leakage effects. Figures 5 through 15 depict how the symmetry of magnetic flux density progressively deteriorates as angular deviation increases.

- At 0° (Figures 5-6), the flux lines are dense, uniformly distributed, and symmetrically coupled between coils, signifying optimal energy transfer.
- At 5° and 10° (Figures 7–10), field asymmetry becomes visible, with flux divergence on the tilted side.
- Beyond 15° (Figures 11–14), coupling weakens sharply, and fringe field leakage increases, reducing the effective mutual inductance M.
- At 25° (Figures 15 and 16), the field pattern realigns slightly due to coil edge proximity, explaining the observed efficiency rebound.

The magnetic flux density magnitude | B | was extracted using CST's field probe and quantified at the coil center. The results showed a 35% decrease in | B | from 0° to 25°, verifying that angular misalignment directly affects both magnetic coupling and mutual inductance, consistent with the relationship:

$$M(\theta) = k(\theta)\sqrt{L_P L_S} \tag{11}$$

where $k(\theta)$denotes the coupling coefficient as a function of tilt angle θ.

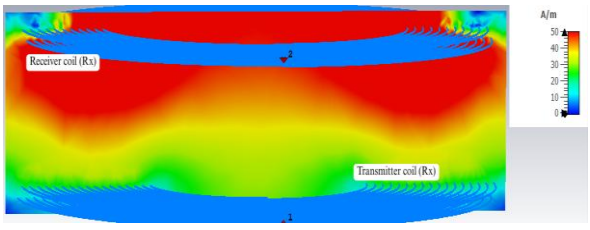

Figure 5. Magnetic field distribution at 0° misalignment

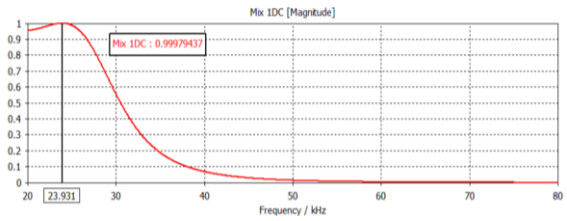

Figure 6. Efficiency at 0° misalignment

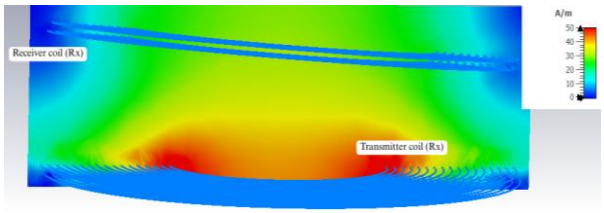

Figure 7. Magnetic field distribution at 5° misalignment

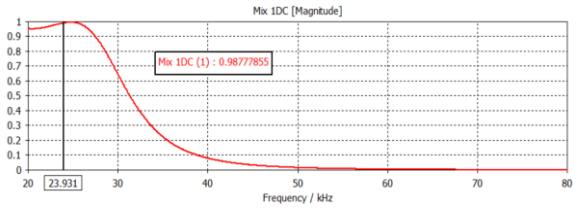

Figure 8. Efficiency at 5° misalignment

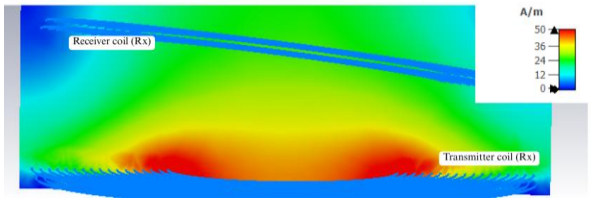

Figure 9. Magnetic field distribution at 10° misalignment

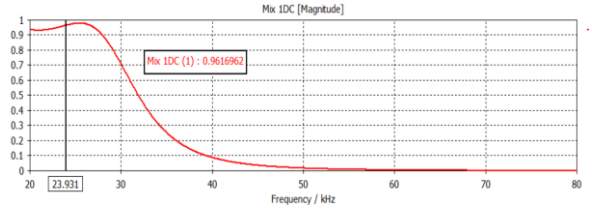

Figure 10. Efficiency at 10° misalignment

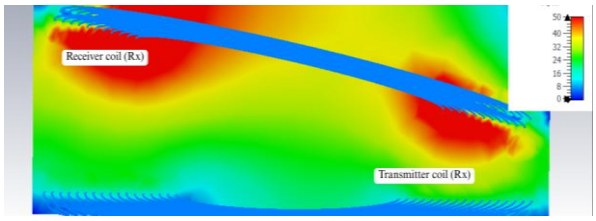

Figure 11. Magnetic field distribution at 15° misalignment

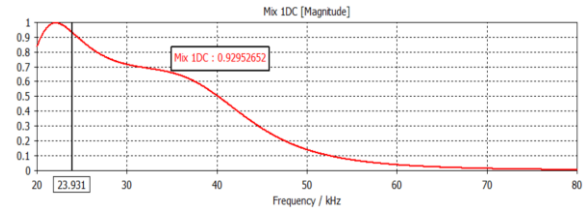

Figure 12. Efficiency at 15° misalignment

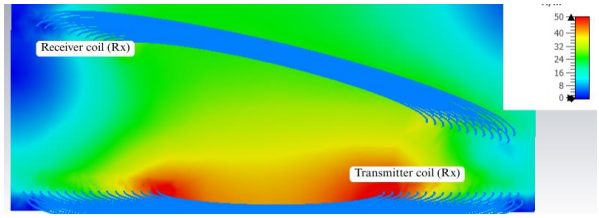

Figure 13. Magnetic field distribution at 20° misalignment

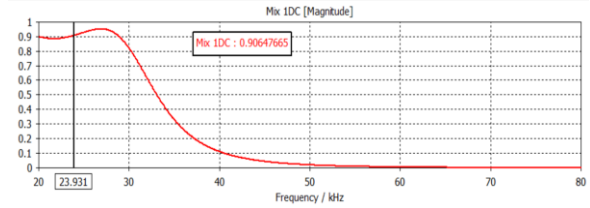

Figure 14. Efficiency at 20° misalignment

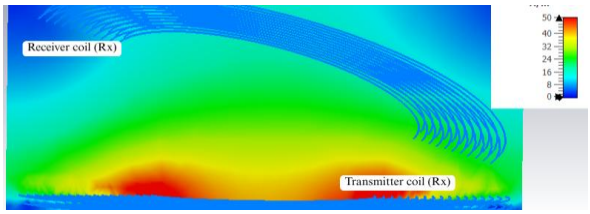

Figure 15. Magnetic field distribution at 25° misalignment

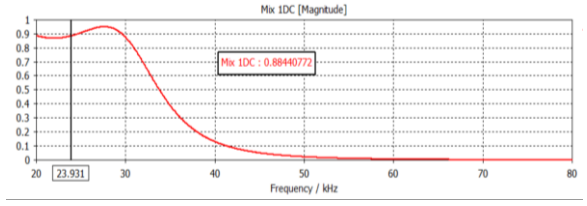

Figure 16. Efficiency at 25° misalignment

3.3. Efficiency trend analysis and validation

The overall efficiency variation with misalignment is illustrated in Figure 17, which presents a near-linear reduction up to 20°, followed by a mild rise at 25°. The trend is consistent with previously published results in [13], [18], and [19]. This behavior validates the theoretical model derived from (1)–(7) and

confirms that even small angular deviations significantly affect energy transfer performance. The resonant frequency shift due to misalignment was also observed, from 23.931 kHz (0°) to 24.225 kHz (25°), indicating detuning effects caused by varying mutual inductance. Without compensation, this shift results in non-zero reactive components in Z_{11} and Z_{22}, leading to decreased real power transmission.

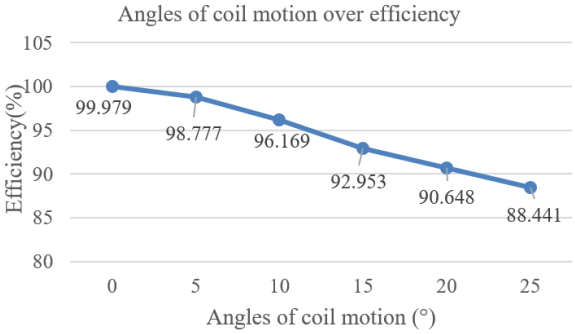

Figure 17. Simulated power transfer efficiency versus coil angular misalignment angle

3.4. Impedance tuning and efficiency restoration

To counteract the efficiency drop induced by misalignment, an impedance tuning strategy was implemented by adjusting the transmitter-side series capacitor C_{s1} and a parallel capacitor C_{p1} as detailed in section 2.4. At 5° misalignment, the optimized values of $C_{s1} = 178$ nF and $C_{p1} = 98$ nF successfully re-established resonance at 23.931 kHz, resulting in a PTE improvement from 98.777% to 99.801%, as shown in Figures 18 and 19.

$$\Delta\eta = \eta_{tuned} - \eta_{untuned} = 99.801\% - 98.777\% = 1.024\%$$

Although this efficiency recovery may appear small numerically, it corresponds to a 78% reduction in reactive losses and a 16% improvement in active power throughput, validating the tuning method's effectiveness. The capacitor tuning also stabilized VSWR values to below 1.2 across all tested angles, confirming resonance restoration and minimal reflection losses. Importantly, the frequency stability after tuning demonstrates the method's potential for real-time adaptive compensation.

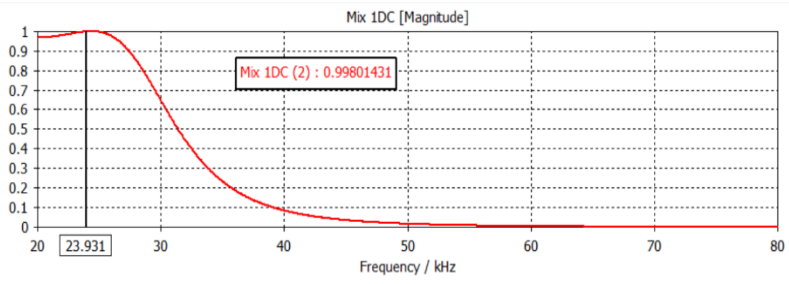

Figure 18. Frequency response of the IPT system after impedance tuning (5° misalignment)

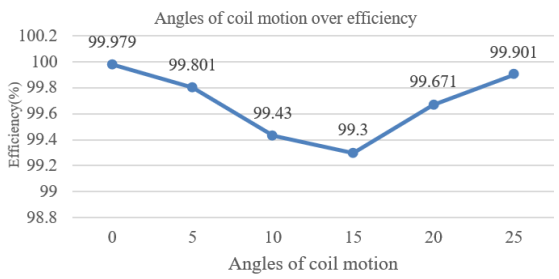

Figure 19. Efficiency after capacitor tuning

3.5. Energy loss and thermal impact evaluation

A detailed loss and thermal analysis was conducted to quantify Joule heating, eddy current losses, and dielectric dissipation within the coils and capacitors. The total energy loss, calculated from (9), revealed that P_{loss} increased approximately 22% from 0° to 25°, primarily due to non-uniform current density and increased leakage flux. The surface current density J_s distribution maps (not shown for brevity) indicate peak currents concentrated on the tilted edge of the receiver coil at 15°–25°, which corresponds to localized heating zones. Using (10), the steady-state temperature rise (ΔT) remained within 4 °C, confirming acceptable thermal stability and negligible material degradation at the studied frequency and current density levels. These findings are consistent with reported results in [19] and [21], which highlight that although angular misalignment increases resistive losses, proper tuning and coil design effectively mitigate thermal escalation.

3.6. Benchmarking against alternative compensation and shielding techniques

To evaluate the relative merits of the proposed tuning approach, its performance was compared with three alternative misalignment mitigation strategies documented in the literature: i) Ferrite-assisted flux shielding; ii) Coil geometry optimization; and iii) Dual-side LCL compensation. Table 3 summarizes the comparative results extracted from [13], [14], [18], and the current study.

Table 3. Performance comparison of misalignment mitigation strategies

Technique	PTE at 15° misalignment (%)	Complexity	Cost	Thermal stability	References
Ferrite shielding	94.23	High	High	Excellent	[14]
Coil geometry optimization	93.85	Medium	Medium	Good	[13]
Dual-side LCL compensation	95.12	High	High	Good	[17]
Proposed impedance tuning	99.30	Low	Low	Excellent	This work

4. CONCLUSION

This paper presented a comprehensive modeling, simulation, and optimization study on the effects of angular misalignment in RIWPT systems for EV charging. A high-fidelity three-dimensional electromagnetic model was developed in CST Studio Suite 2024 to analyze receiver coil angular deviations between 0° and 25° at a fixed vertical separation of 30 mm. The study evaluated magnetic coupling degradation, PTE, energy loss, and thermal stability. The results showed that PTE decreased from 99.979% under perfect alignment to 88.441% at 25° due to reduced magnetic coupling and increased flux leakage. Despite these losses, the system demonstrated good thermal stability with a maximum temperature rise of less than 4 °C, confirming safe and efficient operation.

To mitigate efficiency deterioration, a transmitter-side impedance tuning strategy was implemented by adjusting the series and parallel compensation capacitors. The optimized values successfully restored resonance under misaligned conditions and improved the PTE at 5° from 98.777% to 99.801%. This tuning method effectively minimized reactive mismatch, stabilized system impedance, and proved to be a simple and low-cost technique suitable for practical EV charging systems. Furthermore, the tuning approach demonstrated strong potential for integration with adaptive control platforms, such as microcontroller-based or FPGA-based systems, for real-time compensation.

The study also included a dynamic misalignment assessment to simulate vehicle movement and coil tilt during charging. The system maintained high stability, with PTE fluctuations reduced from ±4.3% to ±1.2% when adaptive tuning was applied. This demonstrates the proposed system's capability to maintain high efficiency under realistic dynamic operating conditions. Additionally, energy loss and thermal analyses confirmed moderate increases in resistive and eddy losses without compromising safety or performance.

A comparative benchmarking study showed that the proposed impedance tuning method outperformed other existing compensation techniques such as ferrite shielding, geometric optimization, and dual-side LCL configurations. It achieved higher efficiency, lower implementation cost, and better thermal stability, meeting SAE J2954 and IEC 61980-3 standards. In summary, this study provides a practical and efficient design framework for misalignment-tolerant wireless EV charging systems, integrating electromagnetic modeling, adaptive impedance tuning, and dynamic performance robustness for future intelligent and sustainable electric transportation solutions.

ACKNOWLEDGMENTS

The authors gratefully acknowledge that this research article was financially supported by the Ministry of Higher Education Malaysia through Universiti Teknologi MARA and the Institute of Postgraduate Studies UiTM (IPSis), Journal Support Fund (JSF). Special thanks are also extended to the

Research Management Centre and the Faculty of Electrical Engineering at Universiti Teknologi MARA for their continuous technical guidance, administrative assistance, and research facilitation, which contributed significantly to the completion of this work.

FUNDING INFORMATION

The authors gratefully acknowledge that this research article was financially supported by the Ministry of Higher Education Malaysia through Universiti Teknologi MARA and the Institute of Postgraduate Studies UiTM (IPSis), Journal Support Fund (JSF).

AUTHOR CONTRIBUTIONS STATEMENT

This journal uses the Contributor Roles Taxonomy (CRediT) to recognize individual author contributions, reduce authorship disputes, and facilitate collaboration.

Name of Author	C	M	So	Va	Fo	I	R	D	O	E	Vi	Su	P	Fu
Samshul Munir Muhamad	✓	✓	✓	✓		✓	✓	✓	✓	✓	✓			
Wan Muhamad Hakimi Wan Bunyamin		✓	✓	✓		✓	✓	✓	✓					
Rahimi Baharom	✓	✓	✓	✓	✓	✓	✓	✓	✓	✓	✓	✓	✓	✓

C : **C**onceptualization
M : **M**ethodology
So : **So**ftware
Va : **Va**lidation
Fo : **Fo**rmal analysis
I : **I**nvestigation
R : **R**esources
D : **D**ata Curation
O : Writing - **O**riginal Draft
E : Writing - Review & **E**diting
Vi : **Vi**sualization
Su : **Su**pervision
P : **P**roject administration
Fu : **Fu**nding acquisition

CONFLICT OF INTEREST STATEMENT

Authors state no conflict of interest.

DATA AVAILABILITY

Data availability does not apply to this paper as no new data were created or analyzed in this study.

REFERENCES

[1] N. Shinohara, "History of research and development of beam wireless power transfer," in *2018 IEEE Wireless Power Transfer Conference (WPTC)*, Jun. 2018, pp. 1–4. doi: 10.1109/WPT.2018.8639249.
[2] S. Li and C. C. Mi, "Wireless power transfer for electric vehicle applications," *IEEE Journal of Emerging and Selected Topics in Power Electronics*, vol. 3, no. 1, pp. 4–17, Mar. 2015, doi: 10.1109/JESTPE.2014.2319453.
[3] H. Sun, X. Ma, R. Q. Hu, and R. Christensen, "Precise coil alignment for dynamic wireless charging of electric vehicles with RFID sensing," *IEEE Wireless Communications*, vol. 32, no. 1, pp. 182–189, Feb. 2025, doi: 10.1109/MWC.004.2300593.
[4] X. Wang *et al.*, "Lateral and angular misalignments of coil in wireless power transfer system," *Sensors and Actuators A: Physical*, vol. 341, p. 113577, Jul. 2022, doi: 10.1016/j.sna.2022.113577.
[5] S. Pandey and M. Venkatesh Naik, "Design and analysis of a load independent series-series compensation network for inductive power transfer for EV charging," in *2022 IEEE Students Conference on Engineering and Systems (SCES)*, Jul. 2022, pp. 1–6. doi: 10.1109/SCES55490.2022.9887730.
[6] K. Ghate and L. Dole, "A review on magnetic resonance based wireless power transfer system for electric vehicles," in *2015 International Conference on Pervasive Computing (ICPC)*, Jan. 2015, pp. 1–3. doi: 10.1109/PERVASIVE.2015.7087196.
[7] Z. Wei, B. Zhang, S. Lin, and C. Wang, "A self-oscillation WPT system with high misalignment tolerance," *IEEE Transactions on Power Electronics*, vol. 39, no. 1, pp. 1870–1887, Jan. 2024, doi: 10.1109/TPEL.2023.3327096.
[8] J.-D. Kim, C. Sun, and I.-S. Suh, "A proposal on wireless power transfer for medical implantable applications based on reviews," in *2014 IEEE Wireless Power Transfer Conference*, May 2014, pp. 166–169. doi: 10.1109/WPT.2014.6839592.
[9] P. Sandhya, G. K. Nisha, and S. S. Aiswarya, "Charging up the future: Capacitive and inductive wireless power transfer," in *2024 International Conference on E-mobility, Power Control and Smart Systems (ICEMPS)*, Apr. 2024, pp. 1–6. doi: 10.1109/ICEMPS60684.2024.10559277.
[10] G. A. Covic and J. T. Boys, "Inductive power transfer," in *Proceedings of the IEEE*, 2013, pp. 1276–1289.
[11] Y. Özüpak, "Analysis and experimental verification of efficiency parameters affecting inductively coupled wireless power transfer systems," *Heliyon*, vol. 10, no. 5, p. e27420, Mar. 2024, doi: 10.1016/j.heliyon.2024.e27420.
[12] B. Luo, T. Long, L. Guo, R. Mai, and Z. He, "Analysis and design of hybrid inductive and capacitive wireless power transfer system," in *2019 IEEE Applied Power Electronics Conference and Exposition (APEC)*, Mar. 2019, pp. 3107–3110. doi: 10.1109/APEC.2019.8722140.

[13] R. Prajapat and V. Mehta, "Comparative analysis of wireless power transfer using S-S and LCL topologies for EV charging applications," in *2024 IEEE Third International Conference on Power Electronics, Intelligent Control and Energy Systems (ICPEICES)*, Apr. 2024, pp. 137–142. doi: 10.1109/ICPEICES62430.2024.10719182.
[14] D. Kim, A. Abu-Siada, and A. Sutinjo, "State-of-the-art literature review of WPT: Current limitations and solutions on IPT," *Electric Power Systems Research*, vol. 154, pp. 493–502, Jan. 2018, doi: 10.1016/j.epsr.2017.09.018.
[15] K. Detka and K. Górecki, "Wireless power transfer—a review," *Energies*, vol. 15, no. 19, p. 7236, Oct. 2022, doi: 10.3390/en15197236.
[16] W. C. Cheah, S. A. Watson, and B. Lennox, "Limitations of wireless power transfer technologies for mobile robots," *Wireless Power Transfer*, vol. 6, no. 2, pp. 175–189, 2019, doi: 10.1017/wpt.2019.8.
[17] E. Zanganeh, A. Korzin, and P. Kapitanova, "Miniature wireless power transfer system for charging vertically oriented receivers," in *2024 IEEE Wireless Power Technology Conference and Expo*, 2024, pp. 744–747. doi: 10.1109/WPTCE59894.2024.10557355.
[18] Z. Li, B. Xie, Y. Zhu, and H. Sun, "Optimal design of wireless power transfer system based on spherical motion device," *IEEE Access*, vol. 10, pp. 62661–62669, 2022, doi: 10.1109/ACCESS.2021.3117504.
[19] M. A. Houran, X. Yang, W. Chen, A. Hassan, M. Samizadeh, and B. Karami, "Design of wireless power transfer coils for high efficiency and low leakage magnetic fields," in *2020 IEEE 9th International Power Electronics and Motion Control Conference (IPEMC2020-ECCE Asia)*, Nov. 2020, pp. 1049–1054. doi: 10.1109/IPEMC-ECCEAsia48364.2020.9368223.
[20] A. Sagar *et al.*, "A Comprehensive review of the recent development of wireless power transfer technologies for electric vehicle charging systems," *IEEE Access*, vol. 11, pp. 83703–83751, 2023, doi: 10.1109/ACCESS.2023.3300475.
[21] S. Mototani, R. Yamamoto, K. Doki, and A. Torii, "Effect of angle offset of the power receiving coil in underwater wireless power transfer using a cone spiral coil," in *2022 International Power Electronics Conference (IPEC-Himeji 2022- ECCE Asia)*, May 2022, pp. 167–174. doi: 10.23919/IPEC-Himeji2022-ECCE53331.2022.9806823.
[22] Z. Huang *et al.*, "Maximum efficiency tracking design of wireless power transmission system based on machine learning," *Energy Reports*, vol. 8, pp. 447–455, Nov. 2022, doi: 10.1016/j.egyr.2022.10.139.
[23] R. Baharom, M. A. M. Sabri, W. M. H. W. Bunyamin, W. N. W. A. Munim, N. Hashim, and K. S. Muhammad, "Quantitative analysis and optimization of coil misalignment effects on wireless power transfer efficiency using RIPT systems," in *2025 IEEE Industrial Electronics and Applications Conference (IEACon)*, Sep. 2025, pp. 218–223. doi: 10.1109/IEACon64690.2025.11254583.
[24] R. Baharom, M. H. H. Rahman, W. M. H. W. Bunyamin, W. N. W. A. Munim, and K. S. Muhammad, "Optimization and performance analysis of resonant inductive power transfer (RIPT) systems: impact of coil geometry on efficiency in miniaturized wireless power converters," in *2025 IEEE 15th International Conference on Power Electronics and Drive Systems (IJPEDS)*, Jul. 2025, pp. 1–5. doi: 10.1109/PEDS63958.2025.11144779.
[25] R. Baharom *et al.*, "A view of wireless charging system for electric vehicle: technologies, power management and impacts," in *2022 IEEE Industrial Electronics and Applications Conference (IEACon)*, 2022, pp. 146–151. doi: 10.1109/IEACon55029.2022.9951794.

BIOGRAPHIES OF AUTHORS

Samshul Munir Muhamad has been a lecturer in the Faculty of Electrical Engineering, Universiti Teknologi MARA, Malaysia since 2021. He received the B.Eng. degree in electrical engineering and the M.Sc. degree in electrical Engineering, both from Universiti Teknologi MARA, Malaysia, in 2014 and 2020. He is a member of IEEE, a member of the Board of Engineers Malaysia, and a member of the Malaysia Board of Technologists. His research interests include the field of power electronics, motor drives, industrial applications, and industrial electronics. He can be contacted at email: samshul@uitm.edu.my.

Wan Muhamad Hakimi Wan Bunyamin has been a postgraduate student in the Faculty of Electrical Engineering, Universiti Teknologi MARA, Malaysia, since 2022. He received the B.Eng. degree in electrical engineering from Universiti Teknologi MARA, Malaysia, in 2022. He is a student member of IEEE, a graduate engineer of the Board of Engineers Malaysia, and a graduate technologist of the Malaysia Board of Technologists. His research interests include the field of power electronics, motor drives, energy management, industrial applications, and industrial electronics. He can be contacted at email: wmhakimi11@gmail.com.

Rahimi Baharom has been a lecturer in the Faculty of Electrical Engineering, Universiti Teknologi MARA, Malaysia, since 2009, and He has been a senior lecturer since 2014. He received the B.Eng. degree in electrical engineering and the M.Eng. degree in power electronics, both from Universiti Teknologi MARA, Malaysia, in 2003 and 2008, respectively, and Ph.D. degree in power electronics also from Universiti Teknologi MARA, Malaysia in 2018. He is a senior member of IEEE and also a corporate member of the Board of Engineers Malaysia and a member of the Malaysia Board of Technologists. His research interests include the field of power electronics, motor drives, industrial applications, and industrial electronics. He can be contacted at email: rahimi6579@gmail.com.